Raman Spectral Conformational Order Indicators in Perdeuterated Alkyl Chain Systems

Zhaohui Liao and Jeanne E. Pemberton*

Department of Chemistry, University of Arizona, 1306 East University Boulevard, Tucson, Arizona 85721

Received: August 25, 2006; In Final Form: November 1, 2006

Conformational order indicators for perdeuterated alkyl chain systems are identified in the Raman spectra of nonadecane-d_{40}, polyethylene-d_4, and stearic acid-d_{35}. Six spectral indicators are identified: $I[\nu_a(CD_2)_{2196}]/I[\nu_a(CD_2)_{2172}]$, $I[\nu(C-C)_G]/I[\nu(C-C)_T]$, $I[\nu_s(CD_3)]/I[\nu_a(CD_2)_{2172}]$, $I[\nu_s(CD_2)]/I[\nu_a(CD_2)_{2172}]$, and the full width at half-maximum (fwhm) and frequency of the $\nu_s(CD_2)$ mode. Among these indicators, the ratio of $I[\nu_a(CD_2)_{2196}]/I[\nu_a(CD_2)_{2172}]$ is considered a primary indicator of conformational order, since it responds to alkyl chain conformational changes in a manner similar to the $I[\nu_a(CH_2)]/I[\nu_s(CH_2)]$ primary indicator for hydrogenated systems. Other indicators are correlated to this primary indicator to derive a better understanding of the effect of structural attributes on conformational order in perdeuterated alkyl chain systems. These Raman spectral order indicators are applicable to any perdeuterated alkyl-containing system including lipids, biological membranes, alkylsilane-based chromatographic stationary phases, and self-assembled monolayers.

Introduction

Raman spectroscopy is a powerful tool for elucidating subtle conformational changes in alkyl chain systems in a variety of chemical environments.[1−10] Spectral indicators of conformational order have been identified in Raman spectral regions containing the $\nu(C-H)$, $\nu(C-C)$, and $\delta(C-H)$ vibrational modes. These indicators provide valuable information about alkyl chain conformational order and interchain coupling which are responsive to relatively subtle molecular structural changes and intermolecular interactions. Despite the success of these approaches, their utility for more complex systems, such as those containing multiple types of alkyl-chain-containing molecules, can be limited by spectral interference with the primary target molecule. Examples of such systems that have relevance to ongoing work in this laboratory[11−19] are alkylsilane stationary phases used in reversed-phase liquid chromatography in the presence of alkyl-containing solutes. In such cases, both the stationary phase and solute will contribute to the response in the Raman spectral regions noted above. This interference is particularly troublesome for solutes that contain long alkyl chains and prohibits independent assessment of stationary phase and solute conformational order.

One common approach to eliminating such interferences is to use one perdeuterated and one hydrogenated alkyl chain system. For example, information about conformational order and packing of alkyl chains in lipid membrane systems is often deduced with Raman spectroscopy. In multicomponent lipid systems, appropriately deuterated lipids have been used as a means of simplifying problems resulting from spectral overlap of individual components.[5,20−24] Hence, it would be highly desirable to identify Raman spectral order indicators in perdeuterated systems with sensitivity to conformational changes comparable to indicators in use for hydrogenated systems. If a collection of such indicators were ascertained, they could allow independent assessment of conformational changes in each component of complex systems such as those described above.

Previous work has identified several Raman spectral indicators of conformational order in deuterated systems. One commonly used indicator is the full width at half-maximum (fwhm) of the $\nu_s(CD_2)$ band at 2103 cm^{-1}.[20−22,25−27] An increase in fwhm corresponds to an increase in the number of gauche conformers along the hydrocarbon chain. Mendelsohn and coworkers[20−22] and Bryant et al.[27] successfully utilized this indicator to study lipid bilayer systems comprised of deuterated phospholipids. Levin later demonstrated that peak intensity ratios often provide more experimentally useful indices than spectral line widths, since the former are easier to construct and are more reproducibly measured in congested spectral regions.[28] On the basis of this work, Levin identified several new empirical spectral order indicators for monitoring interchain and intrachain interactions in deuterated lipid dispersions.[29,30]

Although perdeuterated and selectively deuterated hydrocarbons have been successfully used in such systems to probe conformation, a comprehensive, systematic investigation of Raman spectral order indicators for perdeuterated alkyl-containing systems has not been reported. Toward this end, perdeuterated nonadecane-d_{40} is used here as a model long-chain alkane to systematically identify empirical Raman spectral order indicators of conformational change as a function of temperature. Given that the crystalline-to-liquid transition of nonadecane-d_{40} occurs over a very small temperature range, polyethylene-d_4 is also studied, since its transition is more gradual with temperature. The Raman spectral indicators of order identified from these systems are then successfully applied to study conformation in stearic acid-d_{35}. Finally, spectral order indicators for hydrogenated and deuterated systems are compared.

Experimental

Perdeuterated nonadecane-d_{40} (98%) and stearic acid-d_{35} (98%) were obtained from Cambridge Isotopes. Perdeuterated polyethylene-d_4 (98%, onset melting: 100 °C, melting 130 °C) was obtained from Isotec. All materials were used as received.

Raman spectra were collected using 100 mW of 532.0-nm radiation from a Coherent Verdi Nd:YVO_4 laser (Coherent, Inc.) on a Spex Triplemate spectrograph. Slit settings of the Triplemate were 0.5/7.0/0.15 mm for all experiments, correspond-

* Author to whom correspondence should be addressed.

10.1021/jp0655219 CCC: $33.50
Published on Web 12/08/2006

ing to a spectral bandpass of 5 cm^{-1}. The detector in these experiments was a Princeton Instruments charged-coupled device (CCD) system based on a thinned, back-illuminated, antireflection-coated RTE-110-PB CCD of pixel format 1100 × 330, which was cooled with liquid N_2 to 183 K. Samples were sealed in 5-mm-diameter nuclear magnetic resonance (NMR) tubes and were positioned in the laser beam using a copper sample mount. The temperature of the copper mount was regulated with a 50:50 ethylene glycol:water medium, allowing temperature control from −15 °C to +100 °C. Temperatures greater than 100 °C were obtained by resistively heating the copper sample mount. Samples were allowed to equilibrate at each temperature for a minimum of 30 min prior to analysis to ensure that any temperature-induced changes in conformational order were complete. A minimum of three measurements was made on each sample at each temperature and standard deviations were determined. Error bars are plotted for all data points in the figures. In cases where the error bars are not obvious, they are smaller than the size of the symbol used to indicate the average value. Integration times for each spectrum are provided in the figure captions.

Raw spectral data were background-subtracted using a linear fit of the background in the regions between 1950 and 2350 cm^{-1} and 650 and 1350 cm^{-1}. Peak intensities of the $\nu_a(CD_2)$ and $\nu_s(CD_2)$ bands were determined as peak heights measured from the flat baseline in the resulting spectra. GRAMS 32 was used for decomposition of Raman spectra from nonadecane-d_{40}, polyethylene-d_4, and stearic acid-d_{35} in the liquid state in the ν(C−C) region from 1095 to 1170 cm^{-1} in which the ν-(C−C)$_T$ at 1138 cm^{-1} overlaps the ν(C−C)$_G$ at 1124 cm^{-1}. A 50:50 mixture of Gaussian and Lorentzian functions was used for all peak fittings, as this best fits single-component spectral envelopes more closely than either pure Gaussian or pure Lorentzian functions. The solution was considered to have converged when the reduced χ^2 was minimized and the calculated peak envelope closely matched the experimental peak envelope.

Results and Discussion

Raman Spectral Order Indicators in Hydrogenated Alkyl Chain Systems. Raman spectra in the ν(C−H), ν(C−C), and δ(C−H) regions provide much information about alkyl chain conformational order including degree of chain coupling, chain rotation, and relative amounts of gauche and trans conformers.[1−19] Many empirical Raman spectral indicators of conformational order for hydrogenated systems have been known for almost three decades and are relatively well understood.[1−10] The primary indicator of order is the intensity ratio of the antisymmetric $\nu_a(CH_2)$ band to the symmetric $\nu_s(CH_2)$ band (I[ν_a (CH$_2$)]/I[ν_s (CH$_2$)]). This ratio spans a range from 0.6 to 2.0 for normal alkanes in the liquid (0.6−0.9) and crystalline (1.6−2.0) states[5,10] and is sensitive to subtle changes in conformational order including rotation, twists, kinks, bends of the alkyl chains, and formation of gauche conformers. Thus, it reports any deviation from an all-trans alkyl chain.[3−7] In a recent study from this laboratory, the correlation of additional spectral indicators with this primary indicator was reported for octadecane and a low molecular weight polyethylene (Figure 1). Indicators considered included the peak intensity ratios I[$\nu_s(CH_3)_{FR}$]/I[$\nu_s(CH_2)$] and I[ν(C−C)$_G$]/I[ν(C−C)$_T$], the integrated peak area ratio A[δ_a-(CH$_3$)]/A[δ(CH$_2$)], the peak frequencies of the $\nu_a(CH_2)$, $\nu_s(CH_2)$, and $\tau(CH_2)$ modes, the asymmetry of the $\tau(CH_2)$ mode, and the full width at half-maximum (fwhm) of the $\tau(CH_2)$ mode.[10] For polyethylene, two additional spectral indicators that result from crystal field splitting of the $\delta(CH_2)$ include the peak area ratios A[$\delta_a(CH_3)$]/{A[$\delta(CH_2)$] + A[$\delta(CH_2)_{ORTHO}$]} and A[δ-(CH$_2$)$_{ORTHO}$]/{A[$\delta_a(CH_3)$] + A[$\delta(CH_2)$]}.[10] All indicators were quantitatively correlated to I[$\nu_a(CH_2)$]/I[$\nu_s(CH_2)$], the primary order indicator obtained empirically from the Raman spectra. Subtleties of alkane structure upon melting were investigated providing a definitive molecular picture of this phase change.

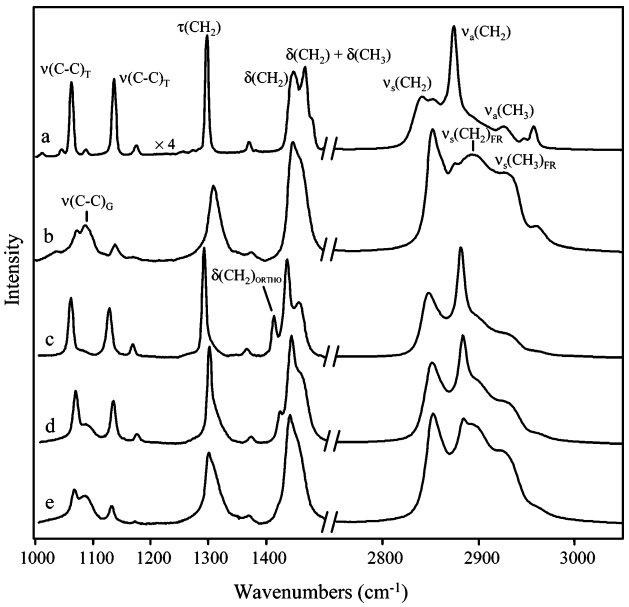

Figure 1. Raman spectra in the ν(C−C) and δ(C−H) regions for octadecane at (a) 0 and (b) 60 °C and for polyethylene at (c) 0, (d) 74, and (e) 100 °C. Integration time 2 min (adapted from ref 10).

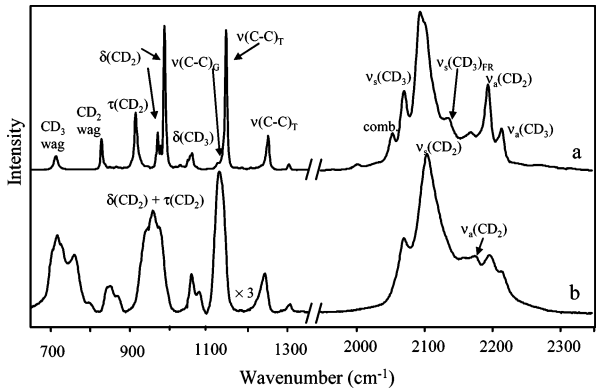

Figure 2. Raman spectra in the ν(C−C) and δ(C−D) regions for nonadecane-d_{40} at (a) 0 and (b) 60 °C. Integration times 2 and 1 min for low- and high-frequency regions, respectively.

General Overview of Conformational Order in Nonadecane-d_{40} and Polyethylene-d_4 from Raman Spectroscopy. Raman spectra in two frequency regions, 650−1350 and 1950−2350 cm^{-1}, from nonadecane-d_{40} at 0 and 60 °C are shown in Figure 2. The corresponding peak frequencies are given in Table 1.[23,31,32] The most intense feature in the 1950−2350 cm^{-1} region is at 2101 cm^{-1}; this feature is composed largely of the methylene $\nu_s(CD_2)$ vibrations of the alkyl chain. The second most intense feature is the band at 2196 cm^{-1}. This mode contains components of both the Raman-active and infrared-active $\nu_a(CD_2)$ modes at 2172 and 2196 cm^{-1}. Its intensity is then sensitive to rotation of the alkyl chains, since Raman-active modes can become infrared-active upon change of symmetry brought about by such rotation.[23] The $\nu_s(CD_3)$ mode is split into two components at 2137 and 2073 cm^{-1} because of Fermi resonance of the fundamental vibration with the overtone of

TABLE 1: Raman Peak Frequencies and Assignments for Nonadecane-d_{40} and Polyethylene-d_4

nonadecane-d_{40}		polyethylene-d_4		
liquid	crystalline	liquid	crystalline	assignments
715 (w)[a]	712 (w)			CD_3 wag
		727 (w)		
759 (w)		759 (w)		
849 (w)	828 (w)	849 (vw)	827 (vw)	CD_2 wag
872 (w)				
937 (w)	913 (m)	937 (w)	914 (w)	$\tau(CD_2)$
	972 (w)		972 (w)	$\delta(CD_2)$
	978 (w)			
	990 (s)		990 (m)	$\delta(CD_2)$
	1056 (w)			$\delta(CD_3)$
		1076 (vw)		
1124 (m)	1124 (vw)	1122 (m)	1124 (vw)	$\nu(C\text{-}C)_G$
1138 (w)	1144 (s)	1138 (w)	1146 (w)	$\nu(C\text{-}C)_T$
1243 (w)		1241 (w)		$\nu(C\text{-}C)_G$
	1250 (w)		1250 (w)	$\nu(C\text{-}C)_T$
	2057 (w)			$\nu(C\text{-}C)_T + \tau(CD_2)$
2073 (m)	2073 (m)	2073 (m)	2073 (m)	$\nu_s(CD_3)$
2106 (s)	2101 (s)	2104 (vs)	2101 (vs)	$\nu_s(CD_2)$
	2137 (m)			$\nu_s(CD_3)_{FR}$
2176 (m)	2172 (w)	2173 (m)	2172 (w)	$\nu_a(CD_2)$
2198 (m)	2196 (m)	2195 (m)	2196 (m)	$\nu_a(CD_2)$
	2216 (w)			$\nu_a(CD_3)$

[a] Relative intensity of each band indicated in parentheses; vs = very strong, s = strong, m = medium, w = weak, vw = very weak. As relative intensities of most bands vary with temperature, intensities indicated correspond to temperatures for each phase as in Figures 2 and 3 for nonadecane-d_{40} and polyethylene-d_4, respectively.

the $\delta(CD_3)$ fundamental at 1056 cm^{-1}. The band at 2216 cm^{-1} is assigned to the $\nu_a(CD_3)$ mode. The band at 2057 cm^{-1} in the crystalline state is tentatively assigned to a combination mode comprising the $\nu(C-C)_T$ mode at 1144 cm^{-1} plus the $\tau(CD_2)$ fundamental at 913 cm^{-1}. However, this assignment is still questionable as will be seen below, since this mode does not show up in the Raman spectra of polyethylene-d_4 and stearic aid-d_{35}, the spectra of which contain both modes. Since the various Fermi resonance interactions that occur in the $\nu(C-H)$ region of hydrogenated alkanes are not relevant to the $\nu(C-D)$ vibrations of nonadecane-d_{40}, the peak height intensity ratios from the Raman bands assigned to the $\nu(C-D)$ modes are not necessarily analogous to the conventional order indicators in the corresponding $\nu(C-H)$ region.[23,29,30]

The intense band in the 650−1350 cm^{-1} region at 1144 cm^{-1} for nonadecane-d_{40} in the crystalline state is assigned to the $\nu(C-C)$ mode of trans conformers, $[\nu(C-C)_T]$. A second $\nu(C-C)_T$ mode is located at 1250 cm^{-1}, which is only ~25% as intense as the 1144 cm^{-1} mode. The shoulders at 1124 and 1243 cm^{-1} in the crystalline state are assigned to $\nu(C-C)_G$ modes.[23,28,30] The $\nu(C-C)_T$ and $\nu(C-C)_G$ modes strongly overlap for nonadecane-d_{40} in the liquid state because of the increasing intensity of the $\nu(C-C)_G$ mode and the shift to slightly lower frequencies of the $\nu(C-C)_T$ mode. Therefore, the broad band in the liquid state centered at 1124 cm^{-1} can be decomposed into contributions from both $\nu(C-C)_T$ and $\nu(C-C)_G$ modes.

Spectral features in the $\delta(C-D)$ region are very complex for nonadecane-d_{40} especially in the liquid state. Several envelopes are observed. The envelope centered at 958 cm^{-1} is comprised of at least the $\tau(CD_2)$ and $\delta(CD_2)$ modes. The $\tau(CD_2)$ mode at 913 cm^{-1} in the crystalline state is broadened and shifted to 937 cm^{-1} in the liquid state, with additional modes appearing on the high-frequency side of this band because of the formation of gauche conformers. This behavior is analogous to that observed for the $\tau(CH_2)$ of hydrogenated systems. The $\delta(CD_2)$ bending and rocking modes exhibit changes in peak intensity, peak width, and frequency. The $\delta(CD_2)$ bending and rocking bands at 972 and 990 cm^{-1}, respectively, shift to slightly lower frequency as well. Although spectral features in the $\delta(C-D)$ region provide qualitative information about alkyl chain conformation, severe band overlap with increasing thermal energy and uncertainty in frequency shifts makes it impossible to accurately extract any quantitative information regarding alkyl chain conformation from this region of the Raman spectrum.

Despite the complexity of the spectral features for nonadecane-d_{40}, six unique Raman spectral indicators can be identified in the $\nu(C-D)$ and $\nu(C-C)$ regions: the peak intensity ratios $I[\nu_a(CD_2)_{2196}]/I[\nu_a(CD_2)_{2172}]$, $I[\nu_s(CD_2)]/I[\nu_a(CD_2)_{2172}]$, $I[\nu_s(CD_3)]/I[\nu_a(CD_2)_{2172}]$, and $I[\nu(C-C)_G]/I[\nu(C-C)_T]$, and the fwhm and peak frequency of the $\nu_s(CD_2)$. These six spectral indicators are further investigated here in an attempt to correlate them with alkyl chain conformational changes and, therefore, with the intermolecular and intramolecular interactions in this perdeuterated alkyl chain system. As shown below, the spectral order indicators identified in this system are generally applicable to other perdeuterated alkyl-containing systems.

Although the $\nu(C-D)$ region (1950−2350 cm^{-1}) is complex for nonadecane-d_{40}, conformational order information can be obtained empirically from the peak intensity ratios $I[\nu_a(CD_2)_{2196}]/I[\nu_a(CD_2)_{2172}]$, $I[\nu_s(CD_2)]/I[\nu_a(CD_2)_{2172}]$, and $I[\nu_s(CD_3)]/I[\nu_a(CD_2)_{2172}]$. Among these three ratios, $I[\nu_a(CD_2)_{2196}]/I[\nu_a(CD_2)_{2172}]$ is the most sensitive across the entire range of achievable conformational states. This ratio ranges from 0.9 to 2.2 across the liquid (0.9−1.1) and crystalline (1.5−2.2) states. It is therefore analogous to $I[\nu_a(CH_2)]/I[\nu_s(CH_2)]$ for hydrogenated systems. $I[\nu_a(CD_2)_{2196}]/I[\nu_a(CD_2)_{2172}]$ is sensitive to subtle changes in conformational order from rotations, kinks, twists, and bends of the alkyl chains, and it also responds to the formation of gauche conformers. In other words, this ratio changes with any deviation of the alkyl chain from a perfect all-trans configuration. Despite its sensitivity to conformational order, it is surprising that this Raman spectral order indicator has never been reported. In contrast, $I[\nu_s(CD_2)]/I[\nu_a(CD_2)_{2172}]$ and $I[\nu_s(CD_3)]/I[\nu_a(CD_2)_{2172}]$ are indicators that are sensitive to alkyl chain coupling. $I[\nu_s(CD_2)]/I[\nu_a(CD_2)_{2172}]$ spans a range from 2.5 to 4.0 for nonadecane-d_{40} across the liquid (2.5−3.0) and crystalline (3.5−4.0) states, whereas $I[\nu_s(CD_3)]/I[\nu_a(CD_2)_{2172}]$ spans a range from 1.1 to 2.1 for nonadecane-d_{40} across the liquid (1.1−1.4) and crystalline (1.7−2.1) states. As the most sensitive and straightforward conformational order indicator, $I[\nu_a(CD_2)_{2196}]/I[\nu_a(CD_2)_{2172}]$ is used as the parameter with which all other chain coupling and gauche conformer spectral indicators are quantitatively correlated here.

Other useful order indicators in the $\nu(C-D)$ region include the frequency and fwhm of the $\nu_s(CD_2)$.[20−23,25,26] The overall $\nu_s(CD_2)$ feature broadens asymmetrically toward higher frequency upon melting, while its peak frequency reflects interchain coupling. This mode is observed at 2097−2101 cm^{-1} for nonadecane-d_{40} in the crystalline state, and its frequency increases by 4−9 cm^{-1} in the liquid state. It has been shown previously that the fwhm of the $\nu_s(CD_2)$ reflects the formation of gauche conformers along the alkyl chains in deuterated phosphoslipid systems.[22] This information is confirmed here, as the fwhm of $\nu_s(CD_2)$ is ~30 cm^{-1} for nonadecane-d_{40} in the crystalline state, increasing to ~40−47 cm^{-1} in the liquid state.

Vibrational modes in the $\nu(C-C)$ and $\delta(C-D)$ regions provide information about conformational order as well. The relative number of gauche and trans conformers is indicated by $I[\nu(C-C)_G]/I[\nu(C-C)_T]$. For nonadecane-$d_{40}$, this ratio ranges from ~0.05 in the crystalline state to 1.5−1.8 in the liquid state.

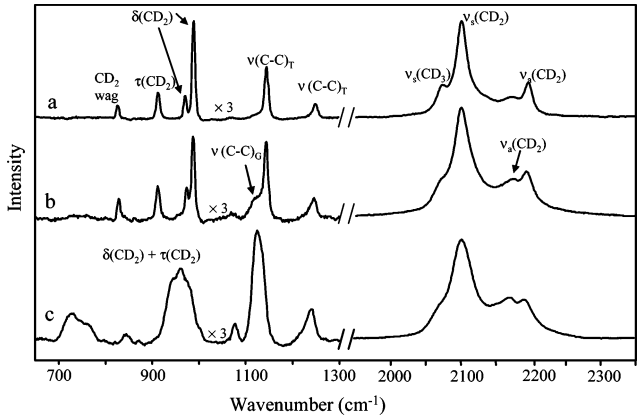

Figure 3. Raman spectra in the ν(C−C) and δ(C−D) regions for polyethylene-d_4 at (a) 0, (b) 120, and (c) 140 °C. Integration times 2 and 1 for low- and high-frequency regions, respectively.

Unlike modes in the ν(C−D) region, the ν(C−C) modes are only sensitive to true gauche and trans conformations and not to methylene rotations.

The phases transition for nonadecane-d_{40} (melting point 27 °C) is abrupt and occurs over an ∼1 °C range, which is typical for a small molecule. As a result, the conformational order information obtained near the melting point is limited by a combination of the kinetics of the transition and the temperature resolution (∼0.5 °C) of the experimental system. Because of the difficulty in controlling the melting event at the phase transition, it is desirable to investigate a system with a more gradual and controllable temperature-induced phase transition so that subtle changes in conformational order through the transition can be studied as well. Toward this end, a low molecular weight perdeuterated polyethylene-d_4 (onset melting: 100 °C, melting point: ∼130 °C) was also investigated.

Raman spectra in the ν(C−D), ν(C−C), and δ(C−D) regions from polyethylene-d_4 at 0, 120, and 140 °C are shown in Figure 3, and the corresponding peak frequencies are given in Table 1. Comparing these spectral data to those of nonadecane-d_{40}, the most obvious differences are the lack of distinct $\nu_a(CD_3)$, $\nu_s(CD_3)_{FR}$, and combination (2057 cm^{-1}) bands in the ν(C−D) region and the lack of distinct $\delta(CD_3)$ wagging and bending modes in the δ(C−D) region. However, all six spectral order indicators identified from nonadecane-d_{40} can also be ascertained from the polyethylene-d_4 system.

Raman Spectral Order Indicators for Nonadecane-d_{40}. The values of $I[\nu_a(CD_2)_{2196}]/I[\nu_a(CD_2)_{2172}]$ and $I[\nu(C-C)_G]/I[\nu(C-C)_T]$ for nonadecane-d_{40} as a function of temperature are shown in Figure 4a and b, respectively. The inset in Figure 4b shows the peak fit of the ν(C−C) region at 70 °C. Each plot is divided by dashed lines into temperature regions corresponding to liquid, biphasic, and crystalline states of nonadecane-d_{40}. As mentioned above, because of the difficulty in temperature control in the phase-transition region, these dashed lines represent approximations of the phase boundaries. The crystalline region ranges from −15 to +26 °C, the biphasic region is in the small window around 27 °C, and the liquid region is from 28 to 90 °C. The $I[\nu_a(CD_2)_{2196}]/I[\nu_a(CD_2)_{2172}]$ clearly reflects changes in conformational order of these alkyl chains with increasing thermal energy. The value of $I[\nu(C-C)_G]/I[\nu(C-C)_T]$ is indicative of the relative number of trans and gauche conformers present in these alky chains at different temperatures.

The correlation between $I[\nu(C-C)_G]/I[\nu(C-C)_T]$ and $I[\nu_a(CD_2)_{2196}]/I[\nu_a(CD_2)_{2172}]$ is shown in Figure 5a. The dashed lines in this figure are approximations of phase boundaries. In the crystalline state, although $I[\nu(C-C)_G]/I[\nu(C-C)_T]$ is relatively constant at 0.05, the conformational order of the alkyl chains decreases as indicated by significant changes in $I[\nu_a(CD_2)_{2196}]/I[\nu_a(CD_2)_{2172}]$. This is thought to be due to the development of end gauche and kink disorder near the ends of a fraction of the alkyl chains. Further into the biphasic region, the average number of gauche conformers increases as indicated by an increase of $I[\nu(C-C)_G]/I[\nu(C-C)_T]$ from 0.2 to 1.4. $I[\nu_a(CD_2)_{2196}]/I[\nu_a(CD_2)_{2172}]$ continues to decrease in this region. In the liquid state, the number of gauche conformers continues to increase with $I[\nu(C-C)_G]/I[\nu(C-C)_T]$ increasing from ∼1.5 to 1.9. $I[\nu_a(CD_2)_{2196}]/I[\nu_a(CD_2)_{2172}]$ remains relatively constant in this region, suggesting that the statistical maximum of disorder that can be accommodated has been reached. As expected, the disorder responsible for the change of $I[\nu_a(CD_2)_{2196}]/I[\nu_a(CD_2)_{2172}]$ is converted to true gauche conformers in the liquid state. Thus, $I[\nu_a(CD_2)_{2196}]/I[\nu_a(CD_2)_{2172}]$ in deuterated systems is analogous to the $I[\nu_a(CH_2)]/I[\nu_s(CH_2)]$ in hydrogenated systems in that they are both sensitive to any deviation from the all-trans state of the alkyl chains.

The ratio of $I[\nu_s(CD_3)]/I[\nu_a(CD_2)_{2172}]$ is thought to be sensitive to alkyl chain intermolecular interactions[29] and, therefore, reflects the degree of interchain coupling. As chains decouple, the terminal methyl groups experience increased rotational freedom, and therefore, the Fermi resonance interactions between $\nu_s(CD_3)$ fundamentals and the overtone of the $\delta(CD_3)$ mode at 1056 cm^{-1} decrease, leading to a decrease in $I[\nu_s(CD_3)]/I[\nu_a(CD_2)_{2172}]$.

The correlation of alkyl chain coupling, as indicated by $I[\nu_s(CD_3)]/I[\nu_a(CD_2)_{2172}]$, with conformational order, as indicated by $I[\nu_a(CD_2)_{2196}]/I[\nu_a(CD_2)_{2172}]$, is shown in Figure 5b. As this

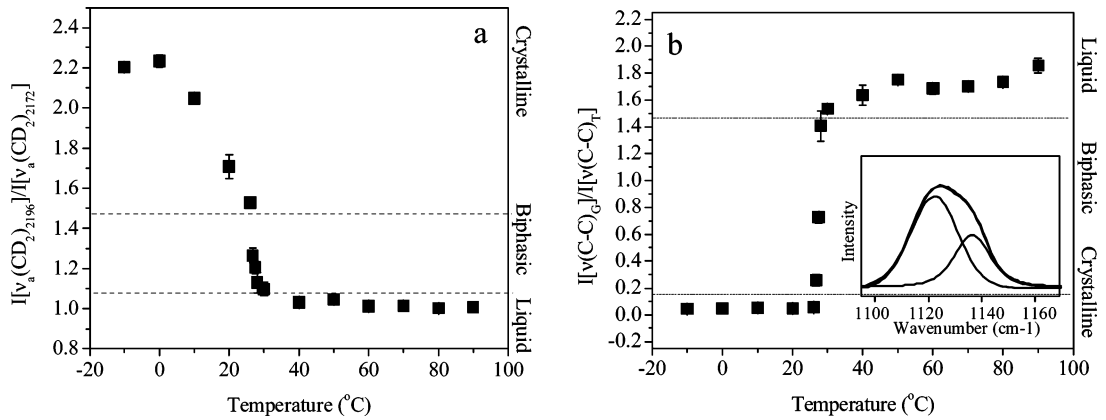

Figure 4. (a) $I[\nu_a(CD_2)_{2196}]/I[\nu_a(CD_2)_{2172}]$ and (b) $I[\nu(C-C)_G]/I[\nu(C-C)_T]$ as a function of temperature for nonadecane-d_{40}. Inset: Peak fit of ν(C−C) mode at 70 °C.

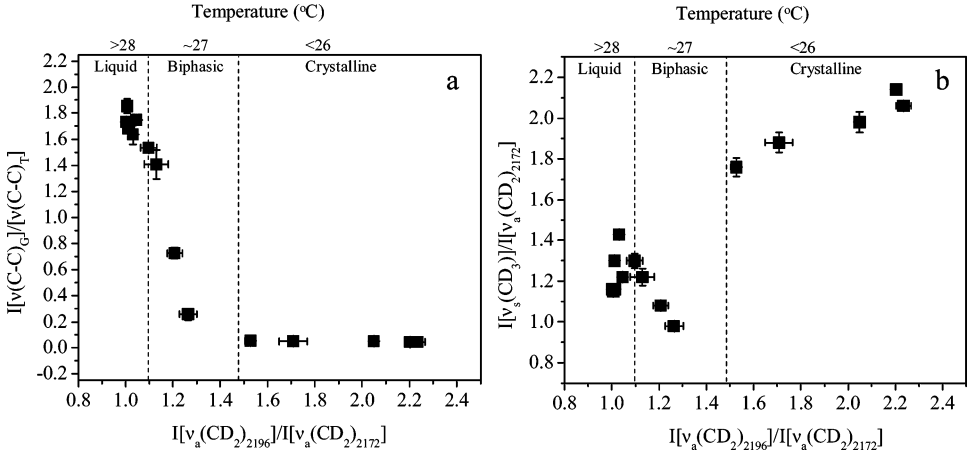

Figure 5. Correlation of (a) $I[\nu(C-C)_G]/I[\nu(C-C)_T]$ with $I[\nu_a(CD_2)_{2196}]/I[\nu_a(CD_2)_{2172}]$ and (b) $I[\nu_s(CD_3)]/I[\nu_a(CD_2)_{2172}]$ with $I[\nu_a(CD_2)_{2196}]/I[\nu_a(CD_2)_{2172}]$ for nonadecane-d_{40}.

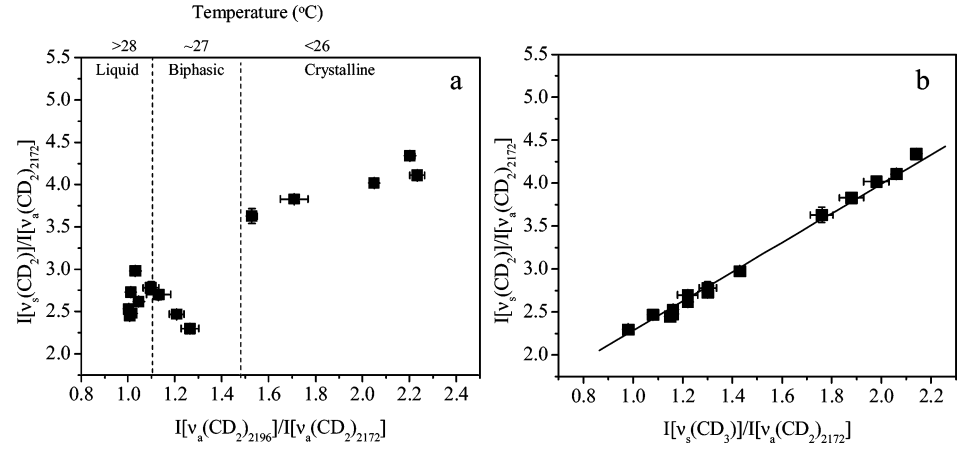

Figure 6. Correlation of (a) $I[\nu_s(CD_2)]/I[\nu_a(CD_2)_{2172}]$ with $I[\nu_a(CD_2)_{2196}]/I[\nu_a(CD_2)_{2172}]$ and (b) $I[\nu_s(CD_2)]/I[\nu_a(CD_2)_{2172}]$ with $I[\nu_s(CD_3)]/I[\nu_a(CD_2)_{2172}]$ (solid line is linear fit; $R^2 = 0.992$) for nonadecane-d_{40}.

plot shows in the crystalline state, interchain coupling decreases with increasing disorder. Through the biphasic and into the liquid states, the chains are sufficiently decoupled to allow gauche conformers to form causing $I[\nu_s(CD_3)]/I[\nu_a(CD_2)_{2172}]$ to decrease substantially and to fluctuate around a value of 1.3. The apparent instability of this ratio may be the result of a combination effect of interchain and intrachain interactions.

As can be seen in Figure 2, the combination band at 2057 cm^{-1} resulting from the $\nu(C-C)_T$ at 1144 cm^{-1} plus the $\tau(CD_2)$ at 913 cm^{-1} is superimposed on the $\nu_s(CH_3)_{FR}$. In the biphasic state, the intensity of the $\nu(C-C)_T$ at 1144 cm^{-1} decreases rapidly and the $\tau(CD_2)$ shifts and broadens considerably, which contribute to the decrease in intensity of the combination band, thereby lowering the intensity of $\nu_s(CH_3)_{FR}$ as measured from the baseline. In the liquid state, however, this combination band shifts to slightly higher frequency because of the upward frequency shift of the $\tau(CD_2)$ mode. Therefore, the $\nu_s(CH_3)_{FR}$ intensity has an additional contribution from this combination band, leading to a slight increase in its intensity. Hence, in the liquid state, $I[\nu_s(CD_3)]/I[\nu_a(CD_2)_{2172}]$ not only reflects interchain coupling, but it is also responsive to a more complex array of structural changes involving gauche conformer formation.

The abrupt phase transition of nonadecane-d_{40} makes distinguishing the effects of intermolecular interactions from the intramolecular effects on $I[\nu_s(CD_3)]/I[\nu_a(CD_2)_{2172}]$ in the biphasic region extremely difficult. As discussed below, investigation of the conformational behavior of polyethylene-d_4 through its more gradual phase transition helps to clarify this ambiguity for nonadecane-d_{40}.

$I[\nu_s(CD_2)]/I[\nu_a(CD_2)_{2172}]$ can also be correlated to $I[\nu_a(CD_2)_{2196}]/I[\nu_a(CD_2)_{2172}]$ as shown in Figure 6a. It resembles the trend observed in the data of Figure 5b for $I[\nu_s(CD_3)]/I[\nu_a(CD_2)_{2172}]$, which suggests that both indicators report the same structural effects. Specifically, the value of $I[\nu_s(CD_2)]/I[\nu_a(CD_2)_{2172}]$ indicates the degree of interchain coupling in the crystalline state; however, in the biphasic and liquid states, this parameter reflects the net effect of alkyl chain intermolecular and intramolecular effects because of the formation of gauche conformers. The linear correlation ($R^2 = 0.992$) between $I[\nu_s(CD_2)]/I[\nu_a(CD_2)_{2172}]$ and $I[\nu_s(CD_3)]/I[\nu_a(CD_2)_{2172}]$ shown in Figure 6b further supports the postulate that they represent identical measures of the same conformational changes. This is not surprising, since the $\nu_s(CD_3)$ is superimposed on the intense $\nu_s(CD_2)$ at 2101 cm^{-1}. Thus, any changes in the intensity of the $\nu_s(CD_3)$ mode lead to a similar change in intensity of the $\nu_s(CD_2)$ mode.

The $\nu_s(CD_2)$ band at 2101 cm^{-1} broadens considerably as the nonadecane-d_{40} goes from the crystalline to liquid state. As a result, the line width of this mode has been used in the past as an indicator of alkyl chain conformational state.[20−23,25−27] Gaber and Peticoclas[6] used isotopic dilution to isolate changes due to gauche formation from those due to interchain effects. From a dilution study involving hexadecane and hexadecane-d_{34}, it was concluded that at least 90% of the change in fwhm

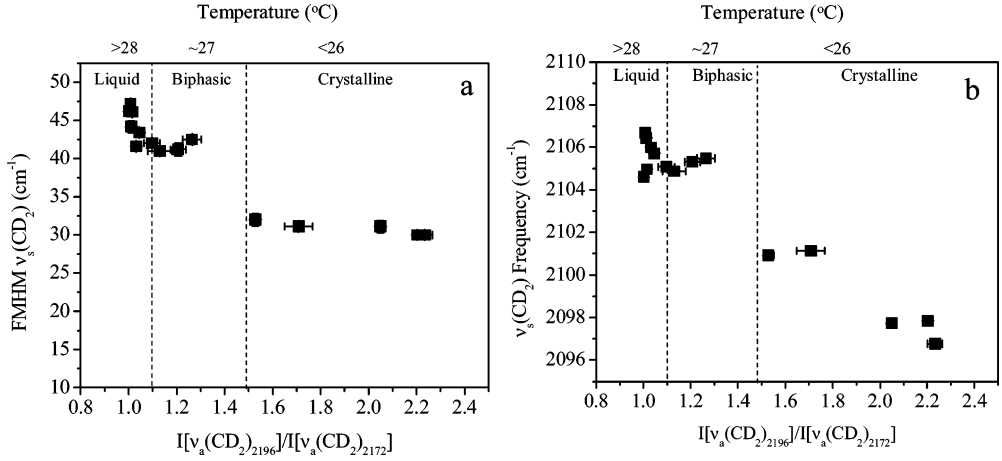

Figure 7. Correlation of (a) $\nu_s(CD_2)$ full width at half-maximum (fwhm) with $I[\nu_a(CD_2)_{2196}]/I[\nu_a(CD_2)_{2172}]$ and (b) $\nu_s(CD_2)$ peak frequency with $I[\nu_a(CD_2)_{2196}]/I[\nu_a(CD_2)_{2172}]$ for nonadecane-d_{40}.

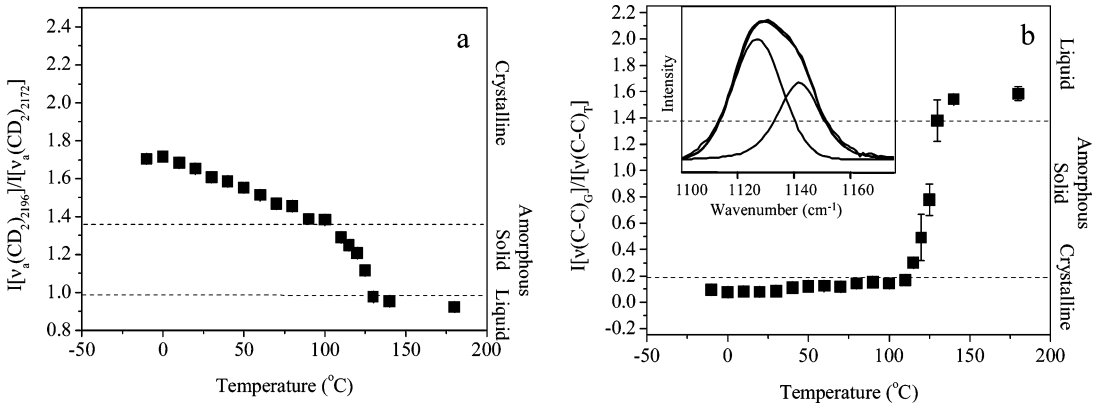

Figure 8. (a) $I[\nu_a(CD_2)_{2196}]/I[\nu_a(CD_2)_{2172}]$ and (b) $I[\nu(C-C)_G]/I[\nu(C-C)_T]$ as a function of temperature for polyethylene-d_4. Inset: Peak fit of $\nu(C-C)$ mode at 140 °C.

of the $\nu_s(CD_2)$ mode reflects the formation of gauche conformers along the hydrocarbon chain.[22] The fwhm of the $\nu_s(CD_2)$ band is correlated to the primary indicator $I[\nu_a(CD_2)_{2196}]/I[\nu_a(CD_2)_{2172}]$ in Figure 7a. In the crystalline state, although the conformational order decreases as indicated by a decrease of $I[\nu_a(CD_2)_{2196}]/I[\nu_a(CD_2)_{2172}]$, the fwhm $\nu_s(CH_2)$ is relatively constant (~30 cm^{-1}), indicating a relatively constant number of gauche conformers. The fwhm of $\nu_s(CD_2)$ rapidly increases to ~40 cm^{-1} in the biphasic state, illustrating the rapid increase in the number of gauche conformers. In the liquid state, the fwhm continues to increase up to ~47 cm^{-1} with a further increase in gauche conformer population.

The correlation between the $\nu_s(CD_2)$ peak frequency, which reflects alkyl chain inter- and intramolecular interactions, and $I[\nu_a(CD_2)_{2196}]/I[\nu_a(CD_2)_{2172}]$ is shown in Figure 7b. In the crystalline state, this frequency is an indicator of interchain coupling, increasing from 2097 to 2101 cm^{-1} because of decoupling of the alkyl chains. In the biphasic and liquid states, the frequency shifts up to 2105 cm^{-1}, reflecting a combination of the increased population of gauche conformers and further decoupling of the alkyl chains.

Raman Spectral Order Indicators for Polyethylene-d_4. Because of the rapid phase transition for nonadecane-d_{40}, it is difficult to obtain spectral information that accurately reflects the conformational change during the transition. Polyethylene-d_4 has an inherent gradual phase transition upon melting that makes it possible to acquire good spectral information during the transition. Moreover, the transition region between crystalline and liquid states for polyethylene-d_4 offers systematically varying disorder, which is useful for understanding the effects of intermolecular interactions and intramolecular effects on the various spectral indicators. Additionally, because of its fewer degrees of freedom[33−35] and a gradual phase transition, polyethyle-d_4 provides a more appropriate model for surface-confined alkane systems.

$I[\nu_a(CD_2)_{2196}]/I[\nu_a(CD_2)_{2172}]$ and $I[\nu(C-C)_G]/I[\nu(C-C)_T]$ as a function of temperature are shown for polyethylene-d_4 in Figure 8a and b, respectively. Each plot is divided into liquid, amorphous solid, and crystalline regions by dashed lines. The crystalline region spans a temperature range from −15 to 100 °C, the amorphous solid region ranges from 100 to 130 °C, and the liquid region is from 130 to 180 °C. The magnitude of $I[\nu_a(CD_2)_{2196}]/I[\nu_a(CD_2)_{2172}]$ clearly reflects changes in conformational order of polyethylene-d_4 with increasing thermal energy, and the $I[\nu(C-C)_G]/I[\nu(C-C)_T]$ is indicative of the relative populations of trans and gauche conformers at different temperatures. Thus, the behavior of these indicators is similar to that observed for nonadecane-d_{40}.

The correlation between $I[\nu(C-C)_G]/I[\nu(C-C)_T]$ and $I[\nu_a(CD_2)_{2196}]/I[\nu_a(CD_2)_{2172}]$ is shown in Figure 9a. In the crystalline state, although the value of $I[\nu(C-C)_G]/I[\nu(C-C)_T]$ increases only slightly from 0.10 to 0.15, the conformational order of the alkyl chains decreases as indicated by the change of $I[\nu_a(CD_2)_{2196}]/I[\nu_a(CD_2)_{2172}]$ from 1.7 to 1.4. Further into the amorphous solid state, the average number of gauche conformers increases as indicated by an increase in $I[\nu(C-C)_G]/I[\nu(C-C)_T]$ from 0.15 to 1.4. The value of $I[\nu_a(CD_2)_{2196}]/I[\nu_a(CD_2)_{2172}]$ in this region also decreases to 1.0. In the liquid state, the number

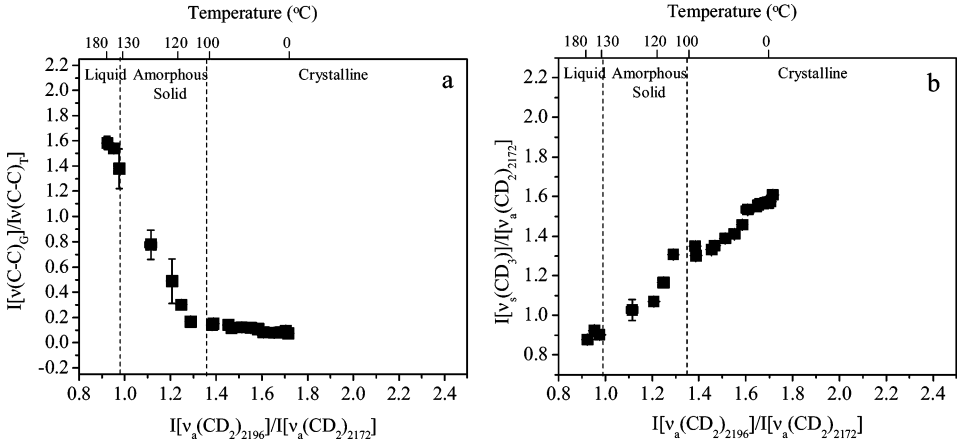

Figure 9. Correlation of (a) $I[\nu(C-C)_G]/I[\nu(C-C)_T]$ with $I[\nu_a(CD_2)_{2196}]/I[\nu_a(CD_2)_{2172}]$ and (b) $I[\nu_s(CD_3)]/I[\nu_a(CD_2)_{2172}]$ with $I[\nu_a(CD_2)_{2196}]/I[\nu_a(CD_2)_{2172}]$ for polyethylene-d_4.

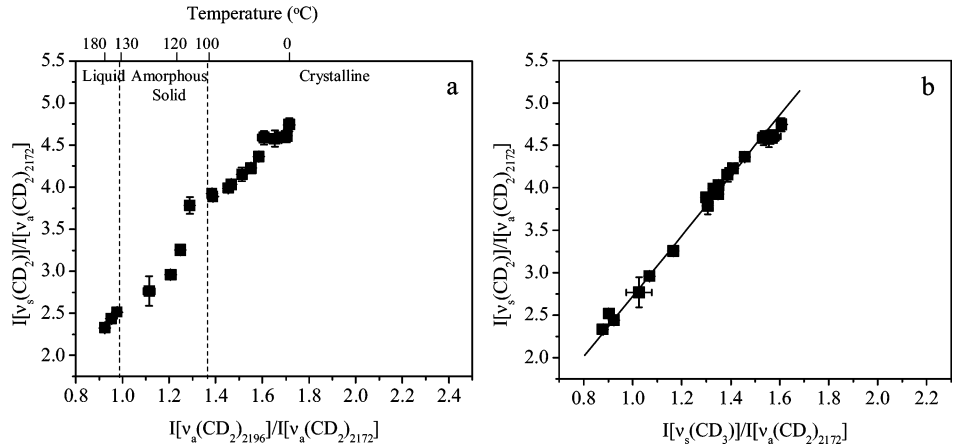

Figure 10. Correlation of (a) $I[\nu_s(CD_2)]/I[\nu_a(CD_2)_{2172}]$ with $I[\nu_a(CD_2)_{2196}]/I[\nu_a(CD_2)_{2172}]$ and (b) $I[\nu_s(CD_2)]/I[\nu_a(CD_2)_{2172}]$ with $I[\nu_s(CD_3)]/I[\nu_a(CD_2)_{2172}]$ ($R^2 = 0.992$) for polyethylene-d_4.

of gauche conformers continues to increase as indicated by an increase of $I[\nu(C-C)_G]/I[\nu(C-C)_T]$ to 1.7, while the value of $I[\nu_a(CD_2)_{2196}]/I[\nu_a(CD_2)_{2172}]$ does not change significantly. The correlation between $I[\nu(C-C)_G]/I[\nu(C-C)_T]$ and $I[\nu_a(CD_2)_{2196}]/I[\nu_a(CD_2)_{2172}]$ for polyethylene-d_4 is similar to that for nonadecane-d_{40}. This correlation further demonstrates that the decrease in $I[\nu_a(CD_2)_{2196}]/I[\nu_a(CD_2)_{2172}]$ is mainly due to the development of methylene conformational disorder. Thus, this indicator is essentially a measure of any deviation from the all-trans state of the alkyl chain. In contrast, increases in $I[\nu(C-C)_G]/I[\nu(C-C)_T]$ are due to the formation of true gauche conformers.

However, in the crystalline state, the magnitudes of both intensity ratios, $I[\nu_a(CD_2)_{2196}]/I[\nu_a(CD_2)_{2172}]$ and $I[\nu(C-C)_G]/I[\nu(C-C)_T]$, for polyethylene-$d_4$ are different than those for nonadecane-d_{40}. Specifically, in the crystalline range, the value of $I[\nu_a(CD_2)_{2196}]/I[\nu_a(CD_2)_{2172}]$ spans a range from 1.5 to 2.2 for nonadecane-d_{40} but from 1.4 to 1.7 for polyethylene-d_4. Similarly, the value of $I[\nu(C-C)_G]/I[\nu(C-C)_T]$ is 0.05 for nonadecane-d_{40} but is 0.10−0.15 for polyethylene-d_4. These differences have been observed preciously in the corresponding ratios for hydrogenated octadecane and polyethylene.[10] They were rationalized in terms of the inherent disorder resulting from the orthorhombic crystal structure of polyethylene, in which the polymer chains contain hairpin bends, compared to the hexagonal crystal structure of octadecane.[33−35] Studies have shown that substitution of deuterium for hydrogen leaves a crystal lattice essentially unchanged.[36] Thus, it would be expected that polyethylene-d_4 would exhibit greater inherent disorder than nonadecane-d_{40}.

The correlation of the alkyl chain interchain coupling parameters, $I[\nu_s(CD_3)]/I[\nu_a(CD_2)_{2172}]$ and $I[\nu_s(CD_2)]/I[\nu_a(CD_2)_{2172}]$, with $I[\nu_a(CD_2)_{2196}]/I[\nu_a(CD_2)_{2172}]$ for polyethylene-d_4 are shown in Figures 9b and 10a, respectively. In the crystalline state, both intensity ratios decrease with decreasing $I[\nu_a(CD_2)_{2196}]/I[\nu_a(CD_2)_{2172}]$, indicating interchain decoupling along with alkyl chain conformational disorder. This observation is similar to that observed for nonadecane-d_{40}. However, unlike the fluctuations observed in the biphasic and liquid state for nonadecane-d_{40}, the values of both intensity ratios for polyethylene-d_4 in the amorphous solid and liquid state are stable and well-behaved. This difference is due to the absence of the combination band (2057 cm^{-1}) resulting from the $\nu(C-C)_T$ at 1144 cm^{-1} and the $\tau(CD_2)$ at 913 cm^{-1} in the spectrum of polyethylene-d_4. As a result, the $\nu_s(CD_3)$ and $\nu_s(CD_2)$ peak intensities for polyethylene-d_4 are not as sensitive to increases in gauche conformer population as those for nonadecane-d_{40}. Therefore, unlike these intensity ratios for nonadecane-d_{40}, the ratios for polyethylene-d_4 reflect only changes in interchain coupling, which decrease with a decrease in conformational order. A linear correlation ($R^2 = 0.992$) between these two interchain coupling indicators (Figure 10b) is observed for polyethylene-d_4 as it was for nonadecane-d_{40}.

As noted above, at least 90% of the sensitivity of the fwhm of $\nu_s(CD_2)$ reflects the formation of gauche conformers along the hydrocarbon chain.[22] The fwhm of the $\nu_s(CD_2)$ band is

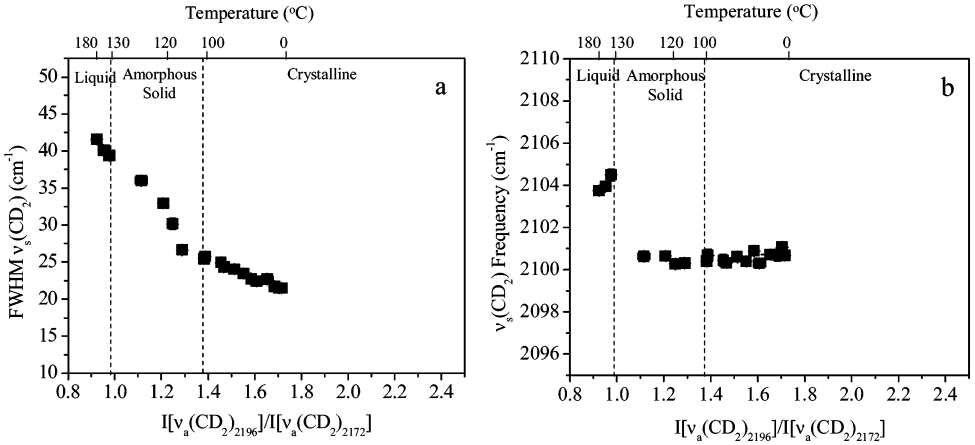

Figure 11. Correlation of (a) $\nu_s(CD_2)$ full width at half-maximum (fwhm) with $I[\nu_a(CD_2)_{2196}]/I[\nu_a(CD_2)_{2172}]$ and (b) $\nu_s(CD_2)$ peak frequency with $I[\nu_a(CD_2)_{2196}]/I[\nu_a(CD_2)_{2172}]$ for polyethylene-d_4.

correlated to the primary indicator $I[\nu_a(CD_2)_{2196}]/I[\nu_a(CD_2)_{2172}]$ in Figure 11a. In the crystalline state, the fwhm of $\nu_s(CD_2)$ increases slightly with increasing $I[\nu_a(CD_2)_{2196}]/I[\nu_a(CD_2)_{2172}]$. This behavior is different from that observed for nonadecane-d_{40} in which the fwhm of $\nu_s(CD_2)$ is relatively constant. However, the increase in fwhm of $\nu_s(CD_2)$ from 22 to 26 cm^{-1} is consistent with the slight increase in number of gauche conformers indicated by $I[\nu(C-C)_G]/I[\nu(C-C)_T]$ which increases from 0.10 to 0.15 (Figure 9a) over this same region. The fwhm of $\nu_s(CD_2)$ rapidly increases to 40 cm^{-1} in the amorphous solid state, indicating a rapid increase in gauche conformer population. In the liquid state, this fwhm continues to increase up to ~42 cm^{-1} with the formation of additional gauche conformers. These results clearly demonstrate that the fwhm of $\nu_s(CD_2)$ is indeed a sensitive indicator of the numbers of gauche conformers in the alkyl chains.

The correlation between $\nu_s(CD_2)$ peak frequency and $I[\nu_a(CD_2)_{2196}]/I[\nu_a(CD_2)_{2172}]$ is shown in Figure 11b. In contrast to the fwhm of the $\nu_s(CD_2)$, the peak frequency mainly reflects alkyl chain coupling in polyethylene-d_4, as it does in hydrogenated alkane systems. In the crystalline and amorphous solid states, the $\nu_s(CD_2)$ frequency is approximately the same (~2101 cm^{-1}), although interchain coupling increases slightly as indicated by the behavior of $I[\nu_s(CD_3)]/I[\nu_a(CD_2)_{2172}]$ (Figure 9b) and $I[\nu_s(CD_2)]/I[\nu_a(CD_2)_{2172}]$ (Figure 10a). It increases further to ~2104 cm^{-1} in the liquid state wherein the interchain distance must increase significantly. Its value remains essentially unchanged in the liquid state.

Application of the spectral order indicators identified in nonadecane-d_{40} and confirmed in polyethylene-d_4 to a third perdeuterated system, stearic acid-d_{35}, is described in the Supporting Information as further evidence of the applicability of these indicators.

Comparison to Hydrogenated Systems. Despite the existence of similar spectral order indicators of conformational order, significant differences exist in the Raman spectra from hydrogenated and perdeuterated alkane systems. Specifically, Fermi resonance splitting due to the interaction of the $\nu_s(CH_2)$ and the overtone of the $\delta(CH_2)$ does not occur in the Raman spectral response of perdeuterated alkyl chains. On the other hand, the combination band resulting from the $\nu(C-C)_T$ and the $\tau(CD_2)$ is not observed in the hydrogenated system. As a result, the conformational order indicators identified for the perdeuterated alkyl chain systems are not strictly analogous to those for hydrogenated systems. Nonetheless, useful indicators exist for both types of systems.

More order indicators are identified in the $\nu(C-D)$ region of perdeuterated systems than in the $\nu(C-H)$ region of hydrogenated systems. However, the primary order indicators for both hydrogenated ($I[\nu_a(CH_2)]/I[\nu_s(CH_2)]$) and perdeuterated ($I[\nu_a(CD_2)_{2196}]/I[\nu_a(CD_2)_{2172}]$) systems are observed in this region. Two other ratios in the $\nu(C-D)$ region, $I[\nu_s(CD_3)]/I[\nu_a(CD_2)_{2172}]$ and $I[\nu_s(CD_2)]/I[\nu_a(CD_2)_{2172}]$, are also observed for the perdeuterated systems that were identified as chain coupling indicators. $I[\nu_s(CD_3)]/I[\nu_a(CD_2)_{2172}]$ for perdeuterated systems behaves in a manner similar to $I[\nu_s(CH_3)_{FR}]/I[\nu_s(CH_2)]$ for hydrogenated systems.

In the $\nu(C-C)$ region, $I[\nu(C-C)_G]/I[\nu(C-C)_T]$ is identified as an indicator of the relative population of gauche conformers for both perdeuterated and hydrogenated systems. These two bands are reasonably well separated in hydrogenated systems. However, in deuterated systems, these two bands are significantly overlapped, requiring spectral decomposition for their use.

The most striking difference between the spectral response for hydrogenated and perdeuterated systems lies in the $\delta(C-H)$ and $\delta(C-D)$ regions. In hydrogenated systems, bands in the $\delta(C-H)$ region are well separated, allowing quantitative determination of changes in the $\tau(CH_2)$ and $\delta(CH_2)$ bands as a function of changes in conformational order. In perdeuterated systems, however, numerous bands appear in this region that all overlap. The number of bands and the characteristics of each band (i.e., peak frequency, peak width, and shape) as a function of temperature are not well-defined preventing determination of any useful order indicators in this region.

Conclusions

This study demonstrates the utility of Raman spectroscopy in determining subtle changes in conformational order and interchain coupling for perdeuterated alkane-containing systems. Six spectral order indicators are identified for perdeuterated alkyl chain systems: $I[\nu_a(CD_2)_{2196}]/I[\nu_a(CD_2)_{2172}]$, $I[\nu(C-C)_G]/I[\nu(C-C)_T]$, $[\nu_s(CD_3)]/I[\nu_a(CD_2)_{2172}]$, $I[\nu_s(CD_2)]/I[\nu_a(CD_2)_{2172}]$, and the fwhm and frequency of the $\nu_s(CD_2)$ mode. These indicators have been successfully applied to three systems investigated here for assessment of conformational order: nonadecane-d_{40}, polyethylene-d_4, and stearic acid-d_{35}. $I[\nu_a(CD_2)_{2196}]/I[\nu_a(CD_2)_{2172}]$ is sensitive to the development of rotational disorder and the formation of small numbers of end gauche and kink conformers in the alkyl chains. It is essentially a measure of any deviation from an all-trans configuration. $I[\nu(C-C)_G]/I[\nu(C-C)_T]$ is indicative of the relative population of gauche conformers. The

magnitudes of $I[\nu_s(CD_3)]/I[\nu_a(CD_2)_{2172}]$ and $I[\nu_s(CD_2)]/I[\nu_a(CD_2)_{2172}]$ and the frequency of the $\nu_s(CD_2)$ represent the degree of alkyl chain coupling. The number of gauche conformers is also reported by the fwhm of the $\nu_s(CD_2)$.

For nonadecane-d_{40} in the crystalline state, thermally induced alkane disorder is developed by decoupling alkyl chains with simultaneous rotational disorder as indicated by the decreasing values of $I[\nu_s(CD_3)]/I[\nu_a(CD_2)_{2172}]$ from 2.1 to 1.1 and $I[\nu_s(CD_2)]/I[\nu_a(CD_2)_{2172}]$ from 4.0 to 3.5, an increase in frequency of the $\nu_s(CD_2)$ from 2097 to 2101 cm^{-1}, and a decrease in $I[\nu_a(CD_2)_{2196}]/I[\nu_a(CD_2)_{2172}]$ from 2.2 to 1.5. The population of gauche conformers is small relative to the numbers of trans conformers in crystalline nonadecane-d_{40} as indicated by the values of $I[\nu(C-C)_G]/I[\nu(C-C)_T]$ (0.05) and the fwhm of the $\nu_s(CD_2)$ (30 cm^{-1}). In the phase-transition region, the rapid development of rotational disorder and the formation of gauche conformers occurs as evidenced by a decrease in $I[\nu_a(CD_2)_{2196}]/I[\nu_a(CD_2)_{2172}]$ from 1.5 to 1.1, an increase in $I[\nu(C-C)_G]/I[\nu(C-C)_T]$ from 0.05 to 1.5, and an increase in fwhm of $\nu_s(CD_2)$ from 30 to 40 cm^{-1}. In the liquid state, rotational disorder continues to increase and converts to true gauche conformers as reflected by the decrease in $I[\nu_a(CD_2)_{2196}]/I[\nu_a(CD_2)_{2172}]$ from 1.1 to 0.9, the increase in $I[\nu(C-C)_G]/I[\nu(C-C)_T]$ from 1.5 to 1.8, and the increase in fwhm of $\nu_s(CD_2)$ from 40 to 48 cm^{-1}. In the phase-transition region and in the liquid state, the degree of alkyl chain coupling should also decrease with increasing thermal energy. However, this decrease in the coupling is not accurately reflected by the values of $I[\nu_s(CD_3)]/I[\nu_a(CD_2)_{2172}]$ or $I[\nu_s(CD_2)]/I[\nu_a(CD_2)_{2172}]$ or the frequency of the $\nu_s(CD_2)$ because of spectral interference. Thus, these interchain coupling indicators should be used with caution for perdeuterated alkanes in the biphasic and liquid states.

Similar changes in conformational order induced by thermal energy occur in the polyethylene-d_4, except that its phase transition is less abrupt than that for nonadecane-d_{40}. In the crystalline state, alkyl chain decoupling and rotational disordering increase with increasing thermal energy as indicated by decreasing values of $[\nu_s(CD_3)]/I[\nu_a(CD_2)_{2172}]$ from 1.6 to 1.3, $I[\nu_s(CD_2)]/I[\nu_a(CD_2)_{2172}]$ from 4.8 to 3.8, and $I[\nu_a(CD_2)_{2196}]/I[\nu_a(CD_2)_{2172}]$ from 1.7 to 1.4. The number of gauche conformers is small relative to the trans conformers present in crystalline polyethylene-d_4 and increases slightly as indicated by increasing values of $I[\nu(C-C)_G]/I[\nu(C-C)_T]$ from 0.1 to 0.15 and the fwhm of the $\nu_s(CD_2)$ from 22 to 26 cm^{-1}. In the phase-transition region, thermally induced rotational disorder and the formation of gauche conformers are indicated by a decrease in $I[\nu_a(CD_2)_{2196}]/I[\nu_a(CD_2)_{2172}]$ from 1.4 to 1.0, an increase in $I[\nu(C-C)_G]/I[\nu(C-C)_T]$ from 0.15 to 1.4, and an increase in fwhm of the $\nu_s(CD_2)$ from 26 to 38 cm^{-1}. The alkyl chains are further decoupled as reflected by decreasing values of $[\nu_s(CD_3)]/I[\nu_a(CD_2)_{2172}]$ from 1.3 to 0.9 and $I[\nu_s(CD_2)]/I[\nu_a(CD_2)_{2172}]$ from 3.8 to 2.5. In the liquid state, as rotational disorder continues to increase and is converted to true gauche conformers, a decrease in $I[\nu_a(CD_2)_{2196}]/I[\nu_a(CD_2)_{2172}]$ from 1.0 to 0.9, an increase in $I[\nu(C-C)_G]/I[\nu(C-C)_T]$ from 1.4 to 1.6, and an increase in the fwhm of $\nu_s(CD_2)$ from 38 to 40 cm^{-1} are observed. In the phase-transition region and in the liquid state, the degree of alkyl chain decoupling should also increase with increasing thermal energy. Although the frequency of the $\nu_s(CD_2)$ responds to the difference in chain coupling between the crystalline and liquid states, increasing from 2101 to 2104 cm^{-1}, it fails to reflect the subtle differences in chain coupling in the crystalline state. Therefore, the frequency of the $\nu_s(CD_2)$ is not as sensitive as the two other chain coupling indicators $[\nu_s(CD_3)]/I[\nu_a(CD_2)_{2172}]$ and $I[\nu_s(CD_2)]/I[\nu_a(CD_2)_{2172}]$.

Thermally induced changes in alkyl chain conformational order and interchain coupling for stearic acid-d_{35} (data and discussion in Supporting Information section) are generally similar to those for nonadecane-d_{40}, except that rapid changes in order and chain coupling are observed for stearic acid-d_{35} just prior to the phase transition. In this state, rotational disordering and the formation of gauche conformers occur as indicated by a decrease in $I[\nu_a(CD_2)_{2196}]/I[\nu_a(CD_2)_{2172}]$ from 1.2 to 1.0 and an increase in both $I[\nu(C-C)_G]/I[\nu(C-C)_T]$ from 0.2 to 1.2 and the fwhm of the $\nu_s(CD_2)$ from 40 to 45 cm^{-1}. The degree of alkyl chain coupling further decreases as reflected by decreasing values of $[\nu_s(CD_3)]/I[\nu_a(CD_2)_{2172}]$ from 1.1 to 0.9 and $I[\nu_s(CD_2)]/I[\nu_a(CD_2)_{2172}]$ from 3.0 to 2.25. In the liquid state, alkyl chain rotational conformers increase and convert to true gauche conformers as indicated by a decrease in $I[\nu_a(CD_2)_{2196}]/I[\nu_a(CD_2)_{2172}]$ from 1.0 to 0.9 as well as an increase in $I[\nu(C-C)_G]/I[\nu(C-C)_T]$ from 1.2 to 1.7 and the fwhm of the $\nu_s(CD_2)$ from 45 to 47 cm^{-1}. Although the degree of chain decoupling continues to increase in the liquid state, $[\nu_s(CD_3)]/I[\nu_a(CD_2)_{2172}]$ and $I[\nu_s(CD_2)]/I[\nu_a(CD_2)_{2172}]$ level off. Therefore, these two chain-coupling indicators are not as sensitive as those for nonadecane-d_{40} and polyethylene-d_4. In addition, similar to that observed for polyethylene-d_4, the frequency of the $\nu_s(CD_2)$ only responds to the difference in interchain coupling between crystalline and liquid states as it increases from ~2101 to 2108 cm^{-1}, but it fails to reflect the subtle differences in chain coupling in the crystalline state. Thus, the frequency of $\nu_s(CD_2)$ as an interchain coupling indicator should be used as caution.

These Raman spectral order indicators can be applied to any perrdeuterated alkane-containing system such as lipids, biological membranes, and self-assembled monolayers on various substrates. It is hoped that the studies described here will help advance the understanding of alkyl chain conformational order and degree of interchain coupling in such systems.

Acknowledgment. The authors gratefully acknowledge support of this research by the Department of Energy (DE-FG03-95ER14546) and the National Science Foundation (CHE-0317114).

Supporting Information Available: Experimental discussion of the investigation of stearic acid-d_{35}. This material is available free of charge via the Internet at http://pubs.acs.org.

References and Notes

(1) Snyder, R. G.; Schachtschneider, J. H. *Spectrochim. Acta* **1963**, *19*, 117.
(2) Spiker, R. C.; Levin, I. W. *Biochim. Biophys. Acta* **1975**, *388*, 361.
(3) Snyder, R. G.; Hsu, S. L.; Krimm, S. *Spectrochim. Acta* **1978**, *34A*, 395.
(4) Snyder, R. G.; Scherer, J. R.; Gaber, B. R. *Biochim. Biophys. Acta* **1980**, *601*, 47.
(5) Wallach, D. F. H.; Varma, S. P.; Fookson, J. *Biochim. Biophys. Acta* **1979**, *559*, 153.
(6) Gaber, B. P.; Peticolas, W. L. *Biochim. Biophys. Acta* **1977**, *465*, 260.
(7) Larson, K.; Rand, R. P. *Biochim. Biophys. Acta* **1973**, *326*, 245.
(8) Snyder, R. G.; Scherer, J. R. *J. Chem. Phys.* **1979**, *71*, 3221.
(9) Synder, R. G.; Strauss, H. L.; Elliger, C. A. *J. Phys. Chem.* **1982**, *86*, 5145.
(10) Orendorff, C. J.; Ducey, M. W.; Pemberton, J. E. *J. Phys. Chem. A* **2002**, *106*, 6991.
(11) Ho, M.; Pemberton, J. E. *Anal. Chem.* **1998**, *70*, 4915.
(12) Doyle, C. A.; Vickers, T. J.; Mann, C. K.; Dorsey, J. G. *J. Chromatogr., A* **2000**, *877*, 25.
(13) Doyle, C. A.; Vickers, T. J.; Mann, C. K.; Dorsey, J. G. *J. Chromatogr., A* **2000**, *877*, 41.

(14) Pemberton, J. E.; Ho, M.; Orendorff, C. J.; Ducey, M. W. *J. Chromatogr., A* **2001**, *913*, 243.
(15) Ducey, M. W.; Orendorff, C. J., Pemberton, J. E.; Sander, L. C. *Anal. Chem.* **2002**, *74*, 5576.
(16) Ducey, M. W.; Orendorff, C. J.; Pemberton, J. E.; Sander, L. C. *Anal. Chem.* **2002**, *74*, 5585.
(17) Orendorff, C. J.; Ducey, M. W.; Pemberton, J. E.; Sander, L. C. *Anal. Chem.* **2003**, *75*, 3360.
(18) Orendorff, C. J.; Ducey, M. W.; Pemberton, J. E.; Sander, L. C. *Anal. Chem.* **2003**, *75*, 3369.
(19) Orendorff, C. J.; Pemberton, J. E. *Anal. Bioanal. Chem.* **2005**, *382*, 691.
(20) Mendelsohn, R.; Maisano, J. *Biochim. Biophys. Acta* **1978**, *506*, 192.
(21) Mendelsohn, R.; Taraschi, T. *Biochemistry* **1978**, *17*, 3944.
(22) Mendelsohn, R.; Koch, C. C. *Biochim. Biophys. Acta* **1980**, *598*, 260.
(23) Bunow, M. R.; Levin, I. W. *Biochim. Biophys. Acta* **1977**, *489*, 191.
(24) Gaber, B. P.; Yager, P.; Peticolas, W. L. *Biophys. J.* **1978**, *22*, 191.
(25) Mendelsohn, R.; Sunder, S.; Bernstein, H. J. *Biochim. Biophys. Acta* **1976**, *443*, 613.
(26) Kawai, T.; Umemura, J.; Takenaka, T. *Chem. Phys. Lett.* **1989**, *162*, 243.
(27) Bryant, G. J.; Lavialle, F.; Levin, I. W. *J. Raman Spectrosc.* **1982**, *12*, 118.
(28) Levin, I. W. In *Advances in Infrared and Raman Spectroscopy*; Clark, R. J. H., Hester, R. E., Eds.; Wiley: New York, 1984; pp 1−48.
(29) Devlin, M. T.; Levin, I. W. *J. Raman Spectrosc.* **1990**, *21*, 441.
(30) McCarthy, P. K.; Huang, C.; Levin, I. W. *Biopolymers (Biospectroscopy*) **2000**, *57*, 2.
(31) Sunder, S.; Mendelsohn, R.; Bernstein, H. J. *Chem. Phys. Lipids* **1976**, *17*, 456.
(32) Boerio, F. J.; Koenig, J. K. *J. Chem. Phys.* **1970**, *52*, 3425.
(33) Boenig, H. V. In *Polyolefins: Structure and Properties*; Elsevier: Amsterdam, 1966.
(34) Keller, A. *Philos. Mag.* **1957**, *2*, 1171.
(35) Niegisch, W. D.; Swan, P. R. *J. Appl. Phys.* **1960**, *31*, 1906.
(36) Kirshenbaum, I. In *Physical Properties and Analysis of Heavy Water*; Urey, H. C., Murphy, G. M., Eds.; McGraw-Hill: New York, 1951; pp 17−18.